Chapter 2 Modeling of a cascaded Raman fiber optic laser

Capítulo 2 Modelización de un láser Raman de fibra óptica en cascada

PAGES-PACHECO, Angeles Yolanda†[1], DE LA CRUZ-MAY, Lelio[1], MEJIA-BELTRAN, Efrain[2] and FLORES-GIL, Aaron[1]

[1]Universidad Autónoma del Carmen, Facultad de Ingeniería, Campus III, Avenida Central S/N, Esq. con Fracc. Mundo Maya, C.P. 24115, Ciudad del Carmen, Campeche, México.
[2]Centro de Investigación en Óptica, Lomas del Bosque 115, Colonia Lomas del Campestre, C.P. 37150, León, Guanajuato, México.

ID 1st Author: *Angeles Yolanda, Pages-Pacheco* / **ORC ID**: 0000-0003-4535-7161, **CVU CONAHCYT ID**: 1005832

ID 1st Co-autor: *Lelio, De la Cruz-May* / **ORC ID**: 0000-0003-3918-0582, **CVU CONAHCYT ID**: 75160

ID 2nd Co-author: *Efraín, Mejía-Beltrán* / **ORC ID**: 0000-0001-8960-6604, **CVU CONAHCYT ID**: 20998

ID 3rd Co-author: *Aaron, Flores-Gil* / **ORC ID**: 0000-0002-2302-2056, **CVU CONAHCYT ID**: 121166

DOI: 10.35429/H.2023.6.9.18

A.Pages, L. De la Cruz, E. Mejía and A. Flores

*institucional 060803@mail.unacar.mx

S. Vargas, S. Figueroa, C. Patiño and J. Sierra (AA. VV.) Engineering and Applied Sciences. Handbooks-TI-©ECORFAN-Mexico, Mexico City, 2023

Abstract

We present a simulation that predicts the phenomenon of Stimulated Raman Scattering (SRS) by continuous wave (CW) laser in silica optical fibers for commercial use in telecommunications. Based on differential equations that describe the generation of Stokes, we also propose a constant that adjusts to the pumping depletion, which is related to Rayleigh backscattering. By introducing this constant into the equations describing the Stokes generation, the results of the numerical simulations approximated the experimental results by 97%.

Numerical modeling, fiber optic Raman laser, SRS, Rayleigh backscattering

Resumen

Presentamos una simulación que predice el fenómeno de la dispersión Raman estimulada (SRS) por láser de onda continua (CW) en fibras ópticas de sílice para uso comercial en telecomunicaciones. Basándonos en ecuaciones diferenciales que describen la generación de Stokes, proponemos también una constante que se ajusta al agotamiento de bombeo, la cual está relacionada con la retrodispersión de Rayleigh. Al introducir esta constante en las ecuaciones que describen la generación de Stokes, los resultados de las simulaciones numéricas se aproximaron en un 97% a los resultados experimentales.

Modelización numérica, Láser Raman de fibra óptica, SRS, Retrodispersión de Rayleigh

Introduction

The Stokes cascade generation in silica optical fibers is a nonlinear process that is based on the Raman process. This happens when radiation from a monochromatic optical light source of a specific wavelength propagates along the optical fiber, where the greatest amount of power is transferred but a small amount is scattered with a new wavelength (commonly 10^{-6}) (Agrawal, 2013). From this Raman scattering, the stimulated Raman scattering (SRS) is generated, which can be understood as the amplification of one of the wavelengths of the spontaneous Raman scattering (Blow & Wood, 1989) (in our study with a shift of ~60nm). This SRS or Stokes, grows like a laser signal and manages to store enough energy to generate spontaneous Raman scattering within the fiber, which with the increase in the power of the pump beam, generates the second Stokes, this successive process generates a Cascading Raman laser.

Fiber Raman lasers in cascades allow efficient laser operation for almost any wavelength, obtaining Stokes components that cover regions applicable to industry, medicine, military, communications, laser spectroscopy and materials processing such as cutting, welding, ablation, among others. (Supradeepa *et al*., 2017). Currently, the generation of a better wavelength shift has been achieved through special fibers with dopants such as boron and germanium, which have a large number of applications since they favor Raman scattering due to their generation of multiple Stokes lines, but They are very difficult to implement, because they have little robustness, poor quality (stability) due to their fragility and are excessively expensive (Mears *et al*., 1985). However, with the appropriate configuration and the correct design it is possible to obtain acceptable results with the use of silica fibers commonly used in telecommunications since they have an efficient Raman gain coefficient, reducing costs in their applications.

Research on the optimization of the Raman laser with silica fiber is very successful and there are analytical equations that describe the phenomenon of energy transfer between the Stokes components and the pump (Islam, 2004), however, a total energy transfer is not achieved. pumping to the first Stokes, but there is a remainder which we call pumping exhaustion. There is still a lack of studies on the effect of pump depletion that cannot be converted into Stokes waves. In various simulations (Vatnik *et al*., 2011, 2012) the energy transfer during the Stokes generation generates a power depletion as indicated (Agrawal, 2013), which does not agree with the published experimental results.

Nowadays, theoretical and experimental studies demonstrate that active media typically exhibit optical phenomena that can significantly affect cascade Raman generation. One of them is Rayleigh backscattering which occurs when a fraction of the light that is scattered is back reflected back to the beginning of the fiber within the optical waveguide (Turitsyn *et al*., 2014).

This can occur in any optical fiber and in all wave bands, having a strong compression effect on the laser linewidth that results in a decrease, broadening and shift of the wavelength in the spectrum of the coupled power after from undergoing Rayleigh backscattering (Zhu *et al*., 2014). Therefore, an adequate study is necessary in the analysis of the set of equations that appropriately predicts the Stokes generation and offers us the possibility of optimizing the laser performance by making fairly good predictions about the energy use of the Raman effect in conventional fibers to manufacture lasers.

In this study, we perform a numerical simulation based on experimental results obtained on commercial silica fibers used in telecommunications. Applying differential equations that predict the generation of Stokes considering the proposal of a constant that limits the power transfer that intervenes between the pumping and the appearance of the Stokes, which is related to Rayleigh backscatter, achieving agreement with the experimental data.

Numerical model

So far, only a few articles have been dedicated to the theoretical description of the properties of fiber Raman lasers. Most of these works present results from numerical modeling of spectral behavior. The simplest model describes the evolution of pump power and signal power along a fiber, z, and can be modeled by coupled equations, respectively. The classical non-cascade SRS process with CW pumping is expressed through the differential equations of Equation (1) (AuYeung & Yariv, 1979; Peng *et al*., 2019):

$$\frac{dP_P^+}{dz} = -\alpha_P P_P^+ - \frac{\upsilon_P}{\upsilon_S}\frac{g_{RP}}{A_{eff}} P_P^+ (P_S^+ + P_S^-)$$

$$\frac{dP_S^+}{dz} = -\alpha_S P_S^+ + \frac{g_{RS}}{A_{eff}} P_S^+ (P_P^+) \quad (1)$$

$$\frac{dP_S^-}{dz} = \alpha_S P_S^- - \frac{g_{RS}}{A_{eff}} P_S^- (P_P^+)$$

Where $P_P^+, P_S^+ \; and \; P_S^-$ represent the pumping and Stokes powers, respectively (superscripts + and – indicate forward and backward propagation);$\alpha_P \; and \; \alpha_S$ are the fiber attenuations for the pump wave and Stokes wave, respectively; $g_{RP} \; and \; g_{RS}$ are the Raman gain coefficients for pumping and Stokes, respectively; *A* represents the effective Stokes area in the fiber and z refers to the position along the axis of the optical fiber.

However, these equations are not sufficient to detail the correct relationship of the SRS, so it is necessary to consider the cascade effect of the Stokes by adding to the previous formulas elements that will develop the energy exchange that occurs between the pumping and the Stokes. An improvement in the approximation of the differential equations would be as follows for 3 Stokes (Ecuación (2)) (Chen *et al*., 2020):

$$\frac{dP_P^+}{dz} = -\alpha_P P_P^+ - \frac{\lambda_{S1}}{\lambda_P}\frac{g_{RP}}{A_{effp}} (P_P^+ - \alpha_{Rp})(P_{S1}^+ + P_{S1}^-)$$

$$\frac{dP_{S1}^+}{dz} = -\alpha_{S1} P_{S1}^+ + \frac{g_{RS1}}{A_{effp}} P_{S1}^+ \left(P_P^+ - \alpha_{Rp}\right) - \frac{g_{RS1}}{A_{effs1}}\frac{\lambda_{S2}}{\lambda_{S1}} (P_{S1}^+ - \alpha_{Rs1})(P_{S2}^+ + P_{S2}^-)$$

$$\frac{dP_{S1}^-}{dz} = \alpha_{S1} P_{S1}^- - \frac{g_{RS1}}{A_{effp}} P_{S1}^- \left(P_P^+ - \alpha_{Rp}\right) + \frac{g_{RS1}}{A_{effs1}}\frac{\lambda_{S2}}{\lambda_{S1}} (P_{S1}^- - \alpha_{Rs1})(P_{S2}^+ + P_{S2}^-)$$

$$\frac{dP_{S2}^+}{dz} = -\alpha_{S2} P_{S2}^+ + \frac{g_{RS2}}{A_{effs1}} P_{S2}^+ (P_{s1}^+ + P_{s1}^- - \alpha_{Rs1}) - \frac{g_{RS2}}{A_{effs2}}\frac{\lambda_{S3}}{\lambda_{S2}} (P_{S2}^+ - \alpha_{Rs2})(P_{S3}^+ + P_{S3}^-) \quad (2)$$

$$\frac{dP_{S2}^{-}}{dz} = \alpha_{S2}P_{S2}^{-} - \frac{g_{RS2}}{A_{effs1}}P_{S2}^{-}(P_{s1}^{+} + P_{s1}^{-} - \alpha_{Rs1}) + \frac{g_{RS2}}{A_{effs2}}\frac{\lambda_{S3}}{\lambda_{S2}}(P_{S2}^{-} - \alpha_{Rs2})(P_{S3}^{+} + P_{S3}^{-})$$

$$\frac{dP_{S3}^{+}}{dz} = -\alpha_{S3}P_{S3}^{+} + \frac{g_{RS3}}{A_{effs2}}P_{S3}^{+}(P_{s2}^{+} + P_{s2}^{-} - \alpha_{Rs2})$$

$$\frac{dP_{S3}^{-}}{dz} = \alpha_{S3}P_{S3}^{-} - \frac{g_{RS3}}{A_{effs2}}P_{S3}^{-}(P_{s2}^{+} + P_{s2}^{-} - \alpha_{Rs2})$$

In this case, the elements were Incorporated $P_{S1}^{+}, P_{S1}^{-}, P_{S2}^{+}, P_{S2}^{-}, P_{S3}^{+}, P_{S3}^{-}$ which correspond to the forward and backward propagation for each of the Stokes; $\lambda_P, \lambda_{s1}, \lambda_{s2}, \lambda_{s3}$ represents the wavelengths at which pumping and Stokes occur; and it was necessary to add the parameter $\alpha_{Rp}, \alpha_{Rs1,}\alpha_{Rs2}$ which represents a factor that limits the energy conversion from the pumping power to the first Stokes, and from this to the next and so on. This Rayleigh backscattering factor is observed experimentally with the shift in the wavelength of the spectrum of the residual power of the pumping, affecting the energy conversion of the residual power by restricting it and preventing it from being completely exhausted during the growth of the first Stokes, it is possible to obtain this value through the experimental results and is unique for each optical fiber with an approximate value of $e^{\wedge(-\alpha L).}$

For the purpose of modeling the SRS, we must consider that increasing the pump power at the entrance of the optical fiber causes the pump beam to generate Raman scattering along the optical fiber, and generally, a great conversion of pump wave to Stokes waves. During this process there are three waves propagating within the fiber: a pump wave that propagates in the forward direction of the beam, which in turn generates a Stokes wave that propagates forward (in the same direction as the beam wave). pump) to the end of the optical fiber and a Stokes wave that propagates backwards, dispersing in the opposite direction to the pump wave due to the influence of the reflectivity at the end of the fiber.

Applying the set of equations (2), a simulation was developed in the Matlab software considering boundary conditions necessary to describe the propagation $P_P^{+}(0) = P_0$, $P_S^{+}(0) = RP_S^{-}(0)$ *and* $P_S^{-}(L) = RP_S^{+}(L)$*;* where R represents the reflectivity of the power at the end of the optical fiber. The analysis process was divided into two stages based on the boundary conditions: the first analyzes the forward propagation of the pump beam from 0 to L and the second analyzes the behavior of the backward propagation from L to 0.

Forward Propagation

This simulation proposes an analysis applying silica fibers commonly used in telecommunications such as the 1060XP fiber and the LEAF to apply it in the design of fiber optic Raman lasers, for this we take into account the length of the optical fiber, the value of the pump power and the parameters provided by the manufacturer such as numerical aperture (NA), core radius (a), fiber attenuation (αt), considering the pumping wavelength and emission of the first and second Stokes (1064nm, 1115nm and 1175nm). From these values and taking the value of the Raman gain previously proposed (de la Cruz-May *et al*., 2013), the simulation stipulates as a starting point the injection of a fictitious photon at z=0 using the following relationship: $P = h\nu B_{eff}$, where h is Planck's constant, ν is the frequency represented by the following relationship $\boldsymbol{\nu = c/\lambda}$ for which c is the speed of light and λ is the wavelength; and B_{eff} is the bandwidth of the effective gain given by Equation (3).

$$B_{eff} = \frac{\Delta V_R}{2}\left[\frac{\pi\alpha_n A_{effn}}{g_n P(z=0)}\right]^{1/2} \qquad \text{B(3)}$$

Because ΔV_R is the full width of the Raman gain and has a value of 13.2 THz, α_n would be the fiber attenuation, g_n is the Raman gain coefficient and A_{effn} is the effective area. Taking into consideration the characteristics and technical parameters provided by the manufacturer of the optical fibers. In the forward SRS we consider initial parameters choosing the backward Stokes waves as zero for the moment. Which are described in Equation 4:

$P_0 = i$; where i is a power interval
$P_1 = h * \upsilon_1 * B_{eff1}$
$P_2 = 0$
$P_3 = h * \upsilon_2 * B_{eff2}$ (4)
$P_4 = 0$
$P_5 = h * \upsilon_3 * B_{eff3}$
$P_6 = 0$

In this case P_1, P_3 and P_5 correspond to the residual pumping power, Stokes 1 and Stokes 2, respectively. These values will serve as a starting point for solving the proposed differential equations, evaluating them in an interval from 0 to L (L refers to the length of the optical fiber).

Back propagation

The next stage in the simulation is to contemplate the propagation of the retroreflected Stokes waves through their path in the fiber from L to 0. Therefore, for this stage new initial values were considered, incorporating the results obtained in Equations (4). and considering the influence of reflectivity during propagation. These are detailed as follows,

$P_{pf} = P_P^+(L)$
$P_{1f} = P_{s1}^+(L)$
$P_{1b} = R\ P_{s1}^+(L)$
$P_{2f} = P_{s2}^+(L)$ (5)
$P_{2b} = R\ P_{s2}^+(L)$
$P_{3f} = P_{s3}^+(L)$
$P_{3b} = R\ P_{s3}^+(L)$

Where P_{pf} is the value of the pump power at the end of the optical fiber, $P_{1f}, P_{2f}\ and\ P_{3f}$ correspond to the power at the output of the optical fiber of the first, second and third Stokes with forward propagation respectively obtained with equations (4) and $P_{1b}, P_{2b}\ and\ P_{3b}$ represents the power at the end of the optical fiber of the first, second and third Stokes with backward propagation respectively. Due to the experimental setup, the reflectivity value is ~4% for all cases where the Stokes wave is retroreflected. Each of these parameters will be analyzed again in the differential equations (2), considering an evaluation of L to 0 as a reference to the fact that all calculations will begin at the end of the optical fiber.

For example, the following figure shows the evolution of the pumping and Stokes powers along the fiber considering the 4% reflectivity, obtained in simulation for a single Stokes in the 1060XP fiber. In Figure 1, it can be seen that the pumping power gradually decreases until it reaches a limit and stops giving up energy, remaining until the exit end of the fiber. When the energy exchange with pumping occurs, Stokes 1 increases slowly until it reaches a maximum energy level and begins to decrease; This process occurs during the forward advancement of power along the distance L in the optical fiber.

However, when analyzing the behavior of the propagation from L to 0 we can observe that the lines that correspond to the backward Stokes have a greater power compared to the forward propagation, this is the same for any of the Stokes that corresponds to what is indicated by the theory and reported by other authors (AuYeung & Yariv, 1979; Vatnik *et al*., 2012). In the case of forward Stokes power, it reaches a maximum energy and subsequently decreases until it is exhausted, while backward Stokes power increases exponentially.

Figure 1 Pump and Stokes propagation within a 1 Km 1060XP fiber with a power of 8W

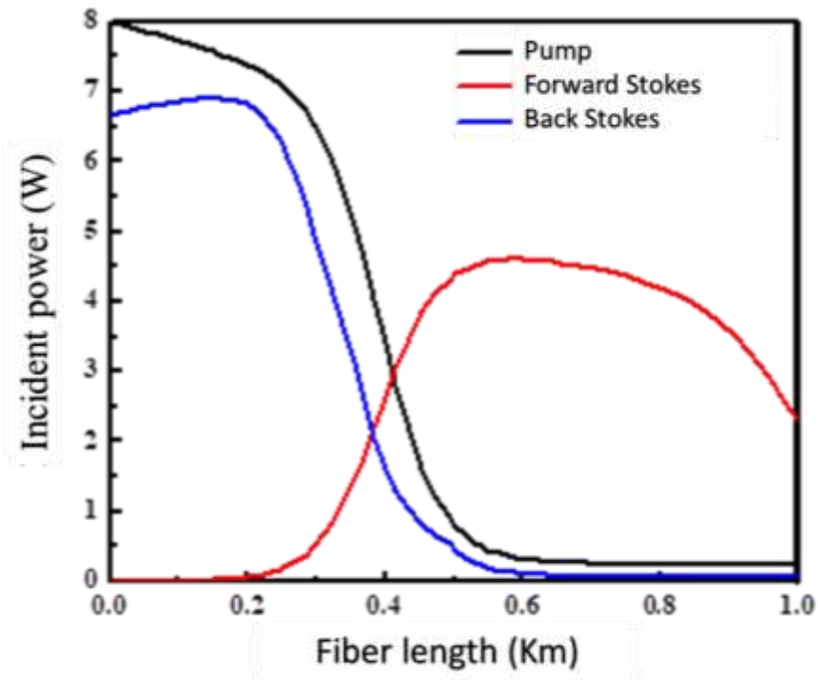

Reference Source: Own Elaboration

Analysis of results

To evaluate the reliability of the data obtained through the simulation, a comparison was made with the experimental results, considering the same technical conditions and the same coupled powers. The results show the evolution of the pumping and Stokes powers along the fiber considering the reflectivity, obtained in simulation.

The simulation provided the data generated by equations (2), managing to obtain the propagation values that were unified as follows $Residual\ power = P_p^+$, Prime Stokes Power ($P_{s1} = P_{s1}^+ + P_{s1}^-$) and Second Stokes Power ($P_{s2} = P_{s2}^+ + P_{s2}^-$) to obtain the final powers at the output of the optical fiber and replicate the Stokes generation.

To corroborate the efficiency of the simulation, two types of silica fibers used in telecommunications were considered: 1060XP and LEAF, both with experimental results already published in (de la Cruz May *et al*., 2023), each with different lengths. As can be seen in Figure 2, each of them was subjected to a special configuration, the LEAF fiber was analyzed under the free running configuration and the 1060XP fiber in a configuration applying Bragg gratings with the aim of speeding up Stokes' generation. Comparing the simulation with these experimental results under specific conditions will allow us to see the scope of the simulation.

Figure 2 Experimental configuration of the study fibers: (A) 9.6 km of LEAF fiber in a free-running configuration, (B) 1 km of 1060XP fiber in a configuration with Bragg gratings

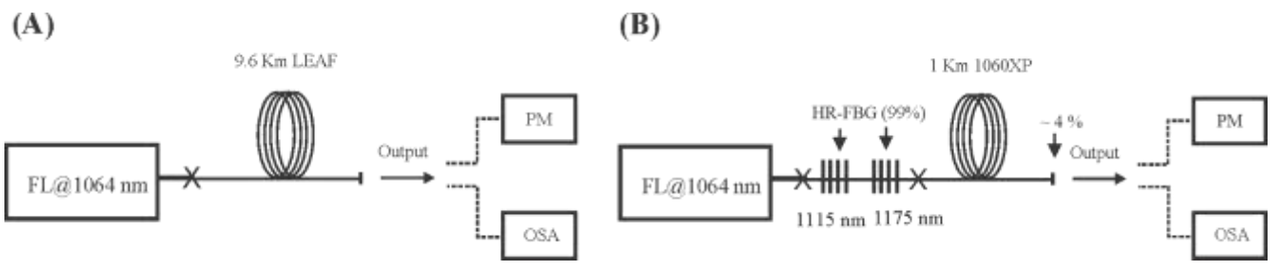

Reference Source: Own Elaboration

Based on the experimental data published on the 1060XP fiber obtained by (de la Cruz May *et al*., 2023; Juárez-Hernández *et al*., 2016) using a coupled power of 8 W it is possible to obtain 2 Stokes as seen in the Graph 1. When comparing with the simulation result, a 92% agreement was achieved in the Stokes generation, but the spectra obtained with the simulation present a small gap with respect to the coupled power. When analyzing pumping depletion, the constant that we introduced in the differential equations (2) was close to 80% in the closest section between the experimental line. However, the simulation for the 1060XP fiber was not able to fully reproduce the experimental results, due to the incorporation of Bragg gratings in the optical fiber, which for the development of the experiment is advantageous due to the faster obtaining of the Stokes generation; however, it causes a delay in pump depletion which could also be due to the limited length of the study fiber which turns out to be very short.

Graphic 1 Comparison of the experimental results with the simulation of the 1060XP fiber (Dashed line: simulation and Solid line: published experimental results) (de la Cruz May *et al*., 2023): Black line corresponds to the pumping power, red to the foreground Stokes and blue to second Stokes

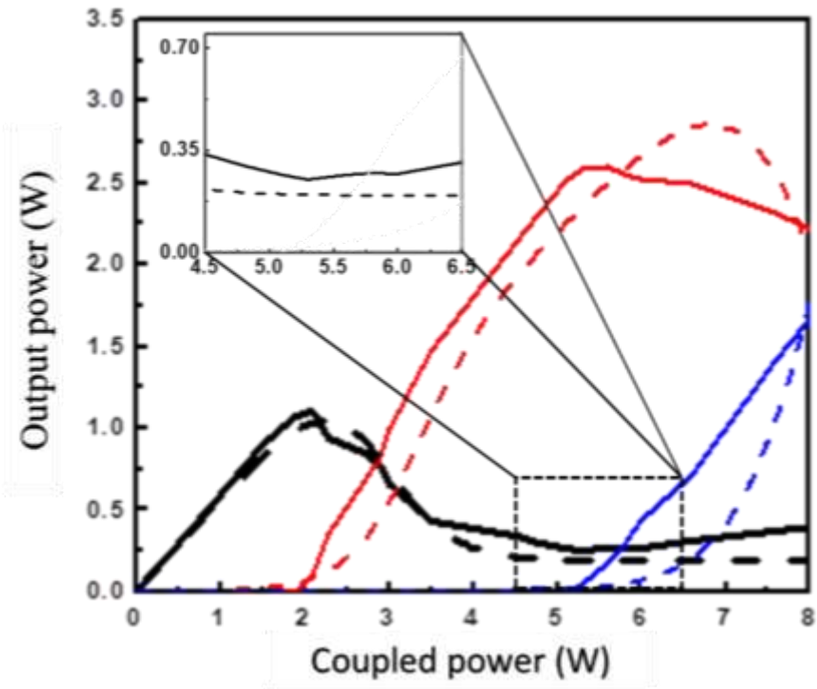

Reference Source:Own Elaboration

In the case study of the LEAF fiber based on the results published in (de la Cruz May *et al*., 2023; Juárez-Hernández *et al*., 2016), a free running configuration was used with a length even longer than in the 1060XP fiber, the comparison with the experimental data and the simulation results contemplates a coupled power of 4 W that allows the generation of the first and second Stokes as can be seen in Graph 2.

Graphic 2 Comparison of the experimental results with the simulation of the LEAF fiber (Dashed line: simulation result and Solid line: published experimental results) (de la Cruz May *et al*., 2023): Black line corresponds to the pumping power, red to the first Stokes and blue to the second Stokes

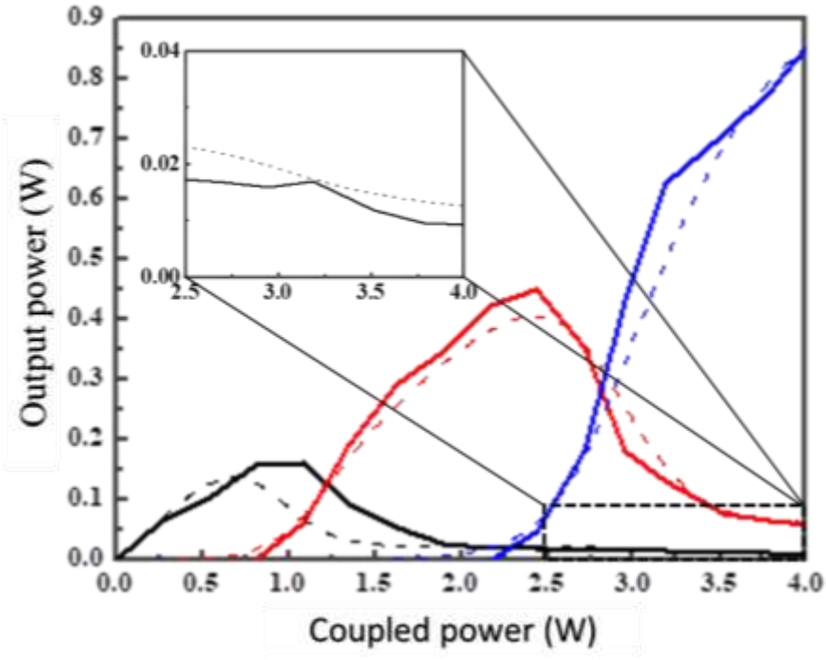

Reference Source: Own Elaboration

With these results, we managed to reproduce the experimental results of Stokes generation for the first and second Stokes. However, there is still a gap with respect to pumping power. The results of the pumping depletion simulation in this study achieved a 99% coincidence in the closest section of the experimental line and the simulation line, considering that the experimental configuration improves the stability of the results and being a fiber of greater length it was possible to observe that not only the transfer of pumping power is restricted but that the exchange of power from the first to the Second Stokes is also affected by Rayleigh backscatter. Therefore, the incorporation of the proposed factor in equations (2) managed to adequately replicate the depletion for pumping and for the successive transfer between the Stokes.

Conclusions

We have presented a simulation that models a fiber optic Raman laser describing the SRS phenomenon, considering the interactions between the pump power with the propagation of Stokes waves towards the end of the optical fiber and the Stokes wave that is retroreflected at the beginning of the fiber. Considering already existing differential equations for the generation of the SRS in cascade for 3 Stokes, a parameter not contemplated in other publications was proposed and incorporated that is related to the influence of Rayleigh backscatter that prevents the pumping power and the Stokes from being exhausted. completely by ceding power to successive Stokes. By comparing the already published experimental results of the 1060XP and LEAF fiber with the results obtained through simulation, trying to replicate the SRS with the appropriate behavior of the power when transferring to the Stokes, it was possible to predict the generation of Stokes in 97% considering both fibers of different lengths, results that will be useful for future analyzes in the design of Raman lasers applying optical fibers for use in telecommunications. Furthermore, by incorporating the proposed parameter into our differential equations, the correct power depletion could be achieved by modeling the published experimental results with good precision, obtaining almost 100% agreement for the LEAF fiber in a free-travel configuration; although the same results could not be achieved for the 1060XP fiber by applying gratings, so it is necessary to continue working to correctly predict the SRS phenomenon for any type of silica fiber. Finally, this set of differential equations can be used to optimize the laser power, offering similar and more realistic results with respect to those obtained experimentally.

References

Agrawal, G. P. (2013). Nonlinear Fiber Optics. In *Nonlinear Science at the Dawn of the 21st Century* (pp. 195–211). Springer Berlin Heidelberg. https://doi.org/10.1007/3-540-46629-0_9 https://opg.optica.org/josab/fulltext.cfm?uri=josab-28-12-A1&id=224263

AuYeung, J., & Yariv, A. (1979). Theory of cw Raman oscillation in optical fibers. *Journal of the Optical Society of America*, *69*(6), 803. https://doi.org/10.1364/JOSA.69.000803 https://opg.optica.org/josa/abstract.cfm?uri=josa-69-6-803

Blow, K. J., & Wood, D. (1989). Theoretical Description of Transient Stimulated Raman Scattering in Optical Fibers. *IEEE Journal of Quantum Electronics*. https://doi.org/10.1109/3.40655 https://ieeexplore.ieee.org/abstract/document/40655

Chen, Y., Yao, T., Xiao, H., Leng, J., & Zhou, P. (2020). Theoretical Analysis of Heat Distribution in Raman Fiber Lasers and Amplifiers Employing Pure Passive Fiber. *IEEE Photonics Journal*, *12*(6), 1–13. https://doi.org/10.1109/JPHOT.2020.3038350 https://ieeexplore.ieee.org/abstract/document/9261093

de la Cruz May, L., Mejia Beltran, E., Benavides, O., Flores Gil, A., Pages Pacheco, A. Y., & Alvarez-Chavez, J. A. (2023). Maximum Pump Power Coupled in Raman Resonator for Maximum Power Delivered at 1115 and 1175 nm. *Photonics*, *10*(5), 531. https://doi.org/10.3390/photonics10050531 https://www.mdpi.com/2304-6732/10/5/531

de la Cruz-May, L., Mejia, E. B., Benavides, O., Vasquez Jimenez, J., Castro-Chacon, J., & May-Alarcon, M. (2013). Novel Technique for Obtaining the Raman Gain Efficiency of Silica Fibers. *IEEE Photonics Journal*, *5*(4), 6100305–6100305. https://doi.org/10.1109/JPHOT.2013.2271900 https://ieeexplore.ieee.org/abstract/document/6552987

Islam, M. N. (2004). Raman amplifiers for telecommunications: physical principles to systems. *Active and Passive Optical Components for WDM Communications IV*. https://doi.org/10.1117/12.580682 https://www.spiedigitallibrary.org/conference-proceedings-of-spie/5595/0000/Raman-amplifiers-for-telecommunications-physical-principles-to-systems/10.1117/12.580682.full?SSO=1

Juárez-Hernández, M., Mejía, E. B., de la Cruz-May, L., & Benavides, O. (2016). Stokes-to-Stokes and anti-Stokes-to-Stokes energy transfer in a Raman fibre laser under different cavity configurations. *Laser Physics*, *26*(11), 115105. https://doi.org/10.1088/1054-660X/26/11/115105 https://iopscience.iop.org/article/10.1088/1054-660X/26/11/115105/meta

Mears, R. J., Reekie, L., Poole, S. B., & Payne, D. N. (1985). Neodymium-Doped Silica Single-Mode Fibre Lasers. *Electronics Letters*. https://doi.org/10.1049/el:19850521 https://ui.adsabs.harvard.edu/abs/1985ElL....21..738M/abstract

Peng, X., Zhang, P., Wang, X., Guo, H., Wang, P., & Dai, S. (2019). Modeling and simulation of a mid-IR 43 μm Raman laser in chalcogenide glass fibers. *OSA Continuum*. https://doi.org/10.1364/osac.2.002281 https://opg.optica.org/osac/fulltext.cfm?uri=osac-2-8-2281&id=415551

Supradeepa, V. R., Feng, Y., & Nicholson, J. W. (2017). Raman fiber lasers. *Journal of Optics*, *19*(2), 023001. https://doi.org/10.1088/2040-8986/19/2/023001 https://iopscience.iop.org/article/10.1088/2040-8986/19/2/023001/meta

Turitsyn, S. K., Babin, S. A., Churkin, D. V., Vatnik, I. D., Nikulin, M., & Podivilov, E. V. (2014). Random distributed feedback fibre lasers. *Physics Reports*, *542*(2), 133–193. https://doi.org/10.1016/j.physrep.2014.02.011 https://www.sciencedirect.com/science/article/abs/pii/S0370157314001215

Vatnik, I. D., Churkin, D. V., & Babin, S. A. (2012). Power optimization of random distributed feedback fiber lasers. *Optics Express*, *20*(27), 28033. https://doi.org/10.1364/OE.20.028033 https://opg.optica.org/oe/fulltext.cfm?uri=oe-20-27-28033&id=246691

Vatnik, I. D., Churkin, D. V., Babin, S. A., & Turitsyn, S. K. (2011). Cascaded random distributed feedback Raman fiber laser operating at 12 μm. *Optics Express*, *19*(19), 18486. https://doi.org/10.1364/OE.19.018486 https://opg.optica.org/oe/fulltext.cfm?uri=oe-19-19-18486&id=222349

Zhu, T., Huang, S., Shi, L., Huang, W., Liu, M., & Chiang, K. (2014). Rayleigh backscattering: a method to highly compress laser linewidth. *Chinese Science Bulletin*, *59*(33), 4631–4636. https://doi.org/10.1007/s11434-014-0603-0 https://link.springer.com/article/10.1007/s11434-014-0603-0